Single-crystal magnetotunnel junctions

W. Wulfhekel,[a] M. Klaua, D. Ullmann, F. Zavaliche, and J. Kirschner
Max-Planck Institut für Mikrostrukturphysik, Weinberg 2, 06120 Halle, Germany

R. Urban, T. Monchesky, and B. Heinrich
Department of Physics, Simon Fraser University, Burnaby, British Columbia, Canada V5A 1S6

(Received 15 August 2000; accepted for publication 21 November 2000)

We have grown epitaxial single-crystal magnetotunnel junctions using Fe(001) substrates, MgO(001) spacers and Fe top electrodes. We have used scanning tunneling microscopy and atomic force microscopy to measure the tunneling characteristics as a function of position and demonstrated that local tunneling can be obtained such that the buried MgO can be characterized with nm resolution. Local $I(V)$ curves revealed that most of the area had intrinsic tunneling properties corresponding to the proper MgO tunneling barrier. A small fraction of the scanned areas showed localized spikes in the tunneling current which are most likely caused by defects in the MgO. © *2001 American Institute of Physics.* [DOI: 10.1063/1.1342778]

Magnetotunnel junctions (MTJs) of high magnetoresistance (MR) at room temperature[1] are a part of an extensive effort to develop magnetic random access memories. The performance of MTJs using polycrystalline electrodes and amorphous Al_2O_3 barriers, however, is governed by resonant tunneling through a large number of poorly understood defects in the barrier.[2] Tunneling proceeds by random hopping, such that the intrinsic properties related to the band structure of the materials are washed away and in addition a strong drop of the magnetoresistance with applied voltage is observed.[3] For single crystalline junctions with perfect insulating barriers, however, the intrinsic tunneling properties can be studied. A magnetoresistance of several hundred percent has been predicted for perfect Fe/MgO/Fe junctions due to band structure effects.[4] MTJs using MgO have enjoyed only limited success. Studies using polycrystalline MgO indicated a low tunneling barrier of ≈ 0.9 eV (Refs. 5–7) pointing at a high density of defects in the barrier. It was shown that one can grow epitaxial films of MgO(001) on Fe(001) substrates.[8,9] Keavney *et al.*[10] prepared crystalline epitaxial Fe/MgO/Fe(001) trilayers using MgO(001) substrates. Unfortunately, pinholes due to a rough bottom Fe layer resulted in shorts in the junction. To allow studies of intrinsic tunneling in crystalline and flat Fe/MgO/Fe junctions, we have grown Fe/MgO/Fe(100) junctions by molecular beam epitaxy (MBE) or pulsed laser deposition (PLD) of MgO and Fe on polished single crystal Fe(100) substrates and Fe whiskers and have characterized the quality of the MgO barrier locally. Fe surfaces were cleaned in ultrahigh vacuum (UHV) by Ar^+ sputtering and annealing[11] until sharp low energy electron diffraction (LEED) patterns were obtained [see Fig. 1(a)] and Auger electron spectroscopy showed only minor contamination by carbon. Scanning tunneling microscopy (STM) images (not shown) revealed flat surfaces with atomic terraces of typically more than 50 nm width for polished surfaces and 1 μm for whiskers. After substrate preparation, MgO was deposited at room temperature in the same UHV chamber by MBE or PLD at a rate of ≈ 1 monolayer (ML)/min. Reflection high energy electron diffraction (RHEED) (not shown) and LEED patterns reveal that MgO grows pseudomorphically on Fe(100) up to 7 ML coverage with MgO[110] parallel to Fe[100] [see Fig. 1(b)], resulting in 3.5% lateral compression of MgO. The LEED spots for MgO and Fe surfaces are equally sharp, with a low background intensity, indicating that the MgO film is crystalline, flat and of high quality. Further, we observe strong RHEED intensity oscillations during both MBE and PLD, indicative of layer-by-layer growth throughout the whole deposition procedure.[12,13] Upon deposition of ≈ 7 ML the strain in MgO is partially released by the formation of misfit dislocations which cause a characteristic splitting of the LEED diffraction peaks.[8,12,13] All MgO thicknesses used in this study were below the onset of misfit dislocations to minimize the effect of lattice defects on tunneling. The height of the tunneling potential barrier in MgO was estimated from ultraviolet photoemission spectra.[12] From the measured energy difference of 4.2 eV between the upper Mg $1s$/O $2p$ valence band edge and the Fermi level of Fe and a 7.8 eV band gap in MgO,[14] a barrier height of 3.6 eV can be estimated.

We have studied the morphology of the MgO films after deposition by STM [see Fig. 2(a)]. The topographic image was taken at 4.2 V such that the electrons tunnel into the conduction band of MgO. The STM image shows, besides the structure of the MgO film, also the structure of the underlying Fe substrate, which displays large monoatomic square vacancy islands due to the preparation by sputtering

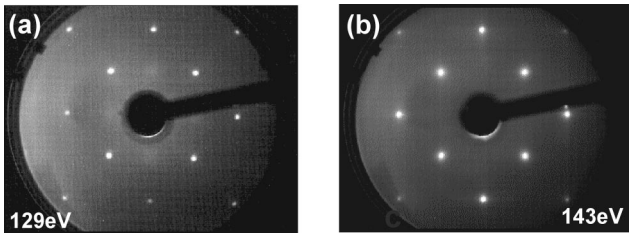

FIG. 1. LEED diffraction spots taken at the energies indicated: (a) clean surface of a Fe(001) whisker; (b) after deposition of 5 ML of MgO(001).

[a]Electronic mail: wulf@mpi-halle.mpg.de

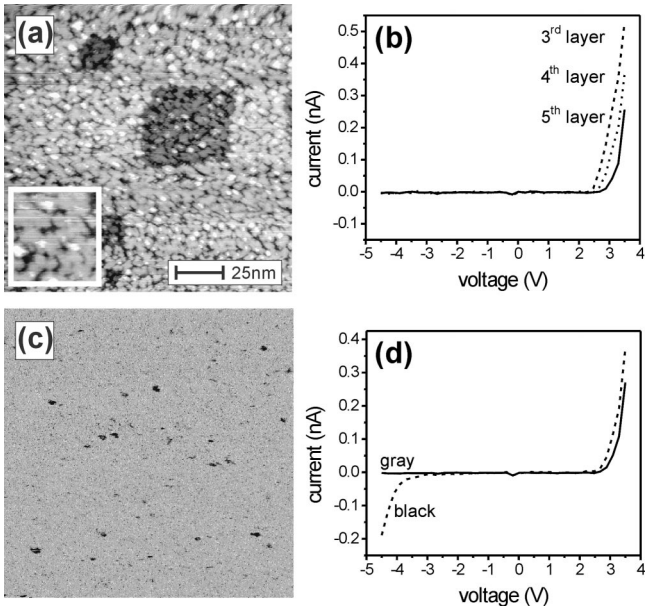

FIG. 2. (a) Morphology of 3.9 ML MgO on Fe(001), (b) tunneling spectra as a function of oxide film thickness, (c) map of the tunneling current of the same area at −4.5 V, and (d) tunneling spectra of low current areas and black spots. STM feedback parameters: 4.2 V, 0.8 nA. The inset of (a) shows the topography magnified by a factor of 2.

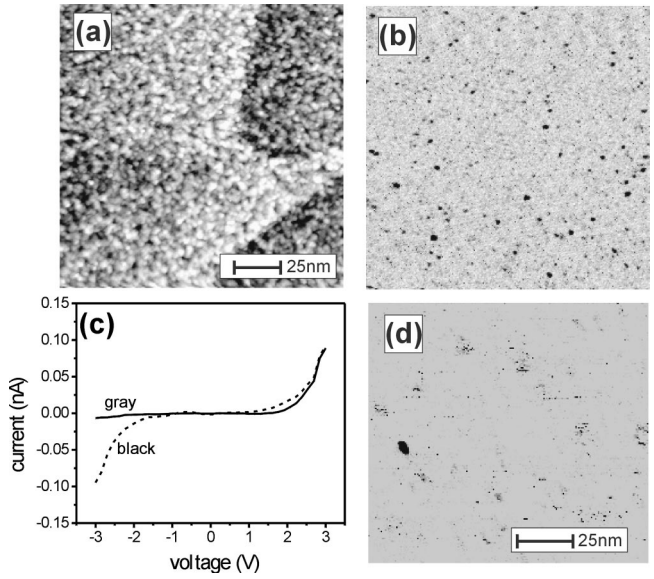

FIG. 3. (a) Morphology of 5 ML Fe on 2 ML MgO on Fe(001), (b) map of the tunneling current of the same area at −3.0 V, and (c) tunneling spectra of low current areas and black spots. STM feedback parameters: (a)–(c) 3.0 V, 0.1 nA. (d) Map of tunneling current at −2 V of 20 ML Au on 20 ML Fe on 4 ML MgO on Fe(001). STM feedback parameters: 1.3 V, 0.4 nA.

and annealing. The small MgO islands show monoatomic steps of the expected height of 0.2 nm and only three open layers at coverage of 3.9 ML. The third atomic layer of the MgO film is completely closed and the fourth is close to completion as expected for layer-by-layer growth at this coverage. Only a small amount of material is found in the fifth layer, indicating a minute deviation from ideal layer-by-layer growth [see also the inset of Fig. 2(a)]. The root mean square (rms) roughness of the film is well below 0.1 nm. The averaged tunneling spectra of the three different ticknesses were taken by STM and are shown in Fig. 2(b). The tunneling spectra are highly asymmetric due to the asymmetry of the tunneling structure. At negative voltages only a small current tunnels from the valence band of MgO into the tip, characteristic of an insulating barrier. At positive voltages just below 4 V the thinner areas show higher currents tunneling from the tip into MgO than the thicker areas, indicative of a lower barrier thickness and/or lower barrier height. A more detailed analysis will be presented elsewhere.[12] We have recorded tunneling spectra for each individual pixel of the STM image of Fig. 2(a), giving a map of the local characteristics of the barrier. Figure 2(c) shows the current at −4.5 V as a function of position. Most of the area shows low currents (displayed in gray). The averaged spectrum of the gray area is displayed in Fig. 2(d). It shows small currents at negative voltages, in agreement with the spectra of the three different thicknesses in Fig. 2(b). A small fraction of the area, however, shows higher currents of up to 200 pA. These areas appear as localized spikes of several nm diameter in the conductance and are plotted in black. They are not correlated with the topography, i.e., they are not related to a locally thinner oxide film. An averaged spectrum of the spikes is displayed in Fig. 2(d). Also at positive voltages, these localized spikes show higher currents. From this we conclude that the spikes are not caused by a thinner oxide film but by a lower tunneling barrier most likely due to localized states in the band gap of the barrier material.

To study the local properties of complete MTJs, we deposited a Fe top electrode onto the insulator either by MBE or PLD. In agreement with the literature,[10] we found with LEED and RHEED that the Fe films grow epitaxially on the MgO film, i.e., fully crystalline MTJs are achieved. Figure 3(a) shows the morphology of the top electrode of 5 ML Fe deposited at room temperature by PLD onto 2 ML MgO. Due to the lower surface free energy of MgO in comparison to that of Fe, the Fe film does not grow in layer-by-layer fashion but shows a somewhat higher rms roughness of ≈ 0.1 nm. Nevertheless, at 5 ML coverage, the Fe film deposited by PLD is completely closed. Interestingly, tunneling spectroscopy on the top electrode also displays local spikes of higher conductance similar to uncovered MgO films [see Fig. 3(b)]. These spots are not related to the topography and are not observed in Fe films deposited directly onto a metal substrate, i.e., the spikes are related to the underlying oxide barrier. In Fig. 3(c) the tunneling spectra at the position of the spikes and of the homogeneous areas are shown. They display the same characteristics as those obtained on the bare MgO. The ability to observe defects in the MgO barrier through the Fe cover points to a considerable fraction of electrons being ballistically transmitted through the Fe film and the buried MgO. If electron transport in the Fe film proceeded entirely diffusively, the tunneling probability and by this the tunneling current would be determined only by the tunneling between the tip and the top electrode. The electrons that tunnel from the tip into the top electrode would diffuse into the conducting top electrode and tunnel in a second step through the MgO at an arbitrary position. No lateral variations of the tunneling spectra should be observed in that case. If, however, there is an additional ballistic channel for the electrons, the properties of the MgO film underneath the tip also determine the total tunneling current and

lateral variations of the tunneling spectra are observed. From the large difference in the local spectra [see Fig. 3(c)] one can conclude that the fraction of the ballistic electrons is considerable. This is in agreement with the low thickness of the top electrode. The hot electrons reaching the MgO film are transmitted through the MgO with a relatively high probability when their energy is close to the local barrier height of MgO. By this, small variations of the local barrier height lead to strong variations of the tunneling current. This mechanism allows the characterization of complete MTJs with thin top electrodes and in principle enables one to study the role of local defects on the MR of MTJs. From mapping of the local currents one can readily conclude that the concentration of defects in the MTJ structure is low. The structures grown are not only of high crystalline quality but also of high electrical quality.

Similar local spikes in the conductance could also be observed, if the Fe/MgO/Fe(001) tunneling junction is covered by 20 ML of Au [see Fig. 3(d)], in agreement with the large mean free path of ballistic electrons in Au of the order of 30 nm.[15] This in principle allows the *ex situ* characterization of junctions that are covered by a thin protective layer against oxidation. In the presented local $I(V)$ measurements, the STM was operated in the constant current mode to first position the tip at a specific distance in front of the top electrode before the feedback loop was opened and the local $I(V)$ spectra were recorded at that fixed tip to sample distance. As a consequence of the positioning of the tip in the constant current mode, all local $I(V)$ spectra go through a common point which is set by the parameters used for stabilizing the tip in the topography mode. Local variations of the conductance are regulated away at this particular voltage and local variations of the oxide barrier only show up in the shape of the $I(V)$ spectra. We alternatively used an AFM with a conducting tip to carry out characterization of gold covered MTJs grown on Fe whiskers.[16] This has the advantage that the spikes in the conductance cannot only be seen in the local $I(V)$ characteristics but also directly in the current at a fixed voltage. During measurements of the tunneling current, the AFM was in dynamic contact mode. At the same time, the current between the conducting tip and the sample was measured. Analogous to the spots observed in tunneling spectroscopy with a STM we found spikes of higher conductance which appear both in variations of the local $I(V)$ spectra and as spikes in the tunneling current at a fixed voltage.[16] However, the transport mechanism of the electrons from the tip into the topmost metallic layer is unclear. A hint about it can be obtained from the shape of the $I(V)$ curves displayed in Fig. 4. The experimental curve can be fitted excellently by hot electrons tunneling through a square barrier[17] of 1.02 ± 0.18 nm width and 3.7 ± 0.1 eV height (see the solid line in Fig. 4), in good agreement with the nominal thickness of the MgO film of 1.05 nm and barrier of 3.6 eV. Assuming that the Fermi level of the top electrode is pulled up by the AFM tip, i.e., Simmons' rule applies,[18] results in a very poor fit of the barrier height of 1.8 ± 0.1 eV and a width of 1.33 ± 0.03 nm. This indicated that most likely the electrons tunnel through a negligible barrier from the AFM tip into the top layer, producing hot electrons in the MTJ.

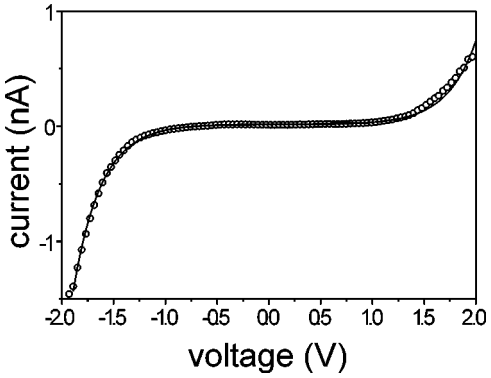

FIG. 4. $I(V)$ spectrum of a Au covered junction with a 5 ML MgO barrier obtained with a conducting AFM tip in dynamic contact mode (circles) and fit using the assumption of hot electrons (solid line).

In conclusion, we have produced single crystalline and flat tunneling junctions and have presented a method by which to study the buried oxide film with tunneling spectroscopy. The density of electronic defects in the barrier is low, indicating high electrical quality of the junctions. This method should be generally applicable to study the quality of the barriers in tunneling junctions, as long as the scattering in the topmost electrode is kept low by using a thin electrode or an electrode of high crystal perfection.

One of the authors (B.H.) acknowledges support by the Alexander von Humboldt Foundation.

[1] J. S. Moodera, L. R. Kinder, T. M. Wong, and R. Meservey, Phys. Rev. Lett. **74**, 3273 (1995).
[2] E. Y. Tsymbal and D. G. Petifor, Phys. Rev. B **58**, 432 (1998).
[3] J. Zhang and R. M. White, J. Appl. Phys. **83**, 6512 (1998).
[4] W. Butler, J. MacLaren, and X. G. Zhang, Phys. Rev. B (in press).
[5] J. S. Moodera and L. R. Kinder, J. Appl. Phys. **79**, 4724 (1996).
[6] C. L. Platt, B. Dieny, and A. E. Berkowitz, J. Appl. Phys. **81**, 5523 (1997).
[7] D. J. Smith, M. R. McCartney, C. L. Platt, and E. E. Berkowitz, J. Appl. Phys. **83**, 5154 (1998).
[8] M. Dynna, J. L. Vassent, A. Marty, and B. Gilles, J. Appl. Phys. **80**, 2650 (1996).
[9] J. L. Vassent, M. Dynna, A. Marty, B. Gilles, and G. Patrat, J. Appl. Phys. **80**, 5727 (1996).
[10] D. J. Keavney, E. E. Fullerton, and S. D. Bader, J. Appl. Phys. **81**, 795 (1997).
[11] B. Heinrich and J. F. Cochran, Adv. Phys. **42**, 523 (1993); B. Heinrich, S. T. Purcell, J. R. Dutcher, K. B. Urquhart, J. F. Cochran, and A. S. Arrot, Phys. Rev. B **38**, 12879 (1988).
[12] M. Klaua (unpublished).
[13] D. Ullman (unpublished).
[14] R. C. Whited, C. J. Flaten, and W. C. Walker, Solid State Commun. **13**, 1903 (1973).
[15] K. M. Weilmeier, W. H. Rippard, and R. A. Buhrman, Phys. Rev. B **59**, R2521 (1999).
[16] T. Monchesky, A. Enders, R. Urban, J. F. Cochran, B. Heinrich, W. Wulfhekel, M. Klaua, F. Zavaliche, and J. Kirschner, *The Physics of Low Dimensions*, edited by J. L. Mraran-Lopez (Plenum, New York, in press).
[17] F. Bardou, Europhys. Lett. **39**, 239 (1997).
[18] J. G. Simmons, J. Appl. Phys. **34**, 1793 (1963).